FRACTURE VARIABILITY OF YTTRIA-STABILIZED ZIRCONIA

D. Casellas, J. Alcalá, L. Llanes and M. Anglada

Departament de Ciència dels Materials i Enginyeria Metal.lúrgica,
ETSEIB, Universitat Politècnica de Catalunya, 08028 Barcelona, SPAIN

ABSTRACT

A fracture model involving the nucleation and growth of circumferential cracks around pre-existing pores is used to compute the fracture strength distribution in a fine-grained zirconia. The application of the model provides a link between the strength variability and the R-curve behavior of the ceramic and its pore size distribution. The results show that the computed Weibull modulus is in good accord with experimental measurements.

INTRODUCTION

Fracture assessments in ceramics are usually conducted considering that the failure is triggered by pre-existing defects, which behave as sharp flaws. This assumption allows one to use concepts from fracture mechanics in the estimation of the fracture strength of ceramic materials. An accurate evaluation of the fracture process in brittle solids requires to study in detail the nucleation and growth of cracks around strength-controlling defects, such as pores, whose relevance to the fracture response has been long recognized [1-3]. Along this lines pores are usually regarded as stress concentrators that promote crack nucleation and the fracture process is then studied using concepts from fracture mechanics.

Different mechanisms are available to increase the fracture toughness in brittle materials. Among others, transformation toughening has long been used to increase the resistance against crack growth in zirconia ceramics. These mechanisms involve a stress-assisted tetragonal to monoclinic ($t \rightarrow m$) phase transformation at the crack tip whose volume increase “shields” the crack from the applied loads. The net result of such transformation toughening effects is the reduction of the effective stress intensity factor, K, at the crack tip.

The objective of this work is to use a fracture model in the estimation of fracture strength variability of a zirconia ceramic from knowledge of its crack growth (R-curve) behavior and pore size distribution. The fracture model is described in detail and it is shown to be useful in bridging the gap between concepts used in structural design with ceramics and more fundamental issues involving the specific crack growth behavior of the these materials.

MATERIAL AND EXPERIMENTAL PROCEDURE

The studied material is an yttria-stabilized zirconia (Y-TZP) formed exclusively by tetragonal grains, with an average size of 0.3 μm. The fracture resistance was evaluated in a previous work (see Ref [3]), where it was shown that the R-curve for this material may be fitted to the following equation

$$K_r = 3.9 + 0.3 \arctan\left(\frac{\Delta a}{29}\right) \quad (1)$$

being Δa the crack extension expressed in μm, and K_r the fracture resistance in MPa√m.

Cylindrical bars of 8 mm in diameter were loaded under three-point bending with a total span of 40 mm. The load was applied at a loading rate of 200 N/s, ensuring that subcritical crack propagation effects were not active. A total of 60 tests were conducted to obtain accurate measurements of the fracture strength distribution from the maximum bending stress of the bar. Prior to testing, all specimens were polished to a 1-μm finish to reduce the influence of machining damage on the strength distribution. The fact that the cylindrical specimens do not contain sharp edges as in the case of square bars is beneficial in ensuring that the fracture response is a unique consequence of the flaw population in the specimen.

Pore size distribution was measured in the polished surface of a total number of 5 different specimens. In doing so, a total cross sectional area of ~ 200 mm^2 was scanned. Due to the minute dimensions of these pores (5-10 μm), measurements were taken from scanning electron microscopy (SEM) micrographs.

FRACTURE MODEL

In view of the observations made on the fracture origins of the fine-grained Y-TZP [3], a reasonable assumption in the fracture model would be that failure originates from circumferential cracks around pores. This is a usual assumption made in ceramics [1,2], as it enables the application of fracture mechanics to the assessment of fracture strength. An important issue in the formulation of the model is whether the small cracks nucleate at elevated temperatures due to, for example, thermal stress mismatch between grains, or if the cracks nucleate at room temperature by the application of external loads in mechanically weak regions around the pores. The underlying reason why the knowledge of the actual crack-nucleating sequence is important in the context of zirconia ceramics is that the amount of phase transformation around the crack would depend on the crack loading history.

In the event that cracks nucleate at *elevated temperatures* due to thermal expansion anisotropy, transformation toughening may not be active since t→m transformation can only occur below a critical temperature. Therefore, a transformation zone around cracks may not be available prior to the application of external loads at room temperature. On the other hand, if the cracks nucleate at room temperature by externally applied loads, transformation toughening would be active throughout the complete crack extension. Due to the anisotropy in thermal expansion coefficient of tetragonal zirconia [4], the assumption of crack nucleation during cooling is reasonable.

If fracture is triggered directly from pores due to stress concentration effects, a numerical analysis of fracture considering the R-curve of the material would be a difficult task as the growth of the “pop-in” crack may be unstable immediately after its nucleation. On the other hand, if prior to the nucleation of the crack, the stresses at the pore surface reach the critical transformation level, another difficulty would be that crack nucleation may occur from pores already surrounded by a transformation zone.

Since it is accepted that fracture of ceramics is usually triggered by pores, it seems important to find out a suitable fracture model that, accounting for this feature, may be able to predict failure. Thus, it is expected that the proposed fracture model may not be particularly demanding on a detailed knowledge of the fracture process, and that the assumptions made in its formulation can be compensated by calibration through fracture experiments. Such calibration will warrant that the model captures the essence of the fracture processes in the Y-TZP under consideration.

The following are the critical assumptions for the model.

- Circumferential cracks originate from pores and their propagation under external loads controls the fracture strength of the material (this is not a new proposition as the assumption that cracks emerge from processing induced pores has been invoked extensively in the past [1,2]). Directing attention to figure 1, the controlling factor in this assumption is the ratio of crack length to pore radius, c/R, which sets the value of the stress intensity factor.

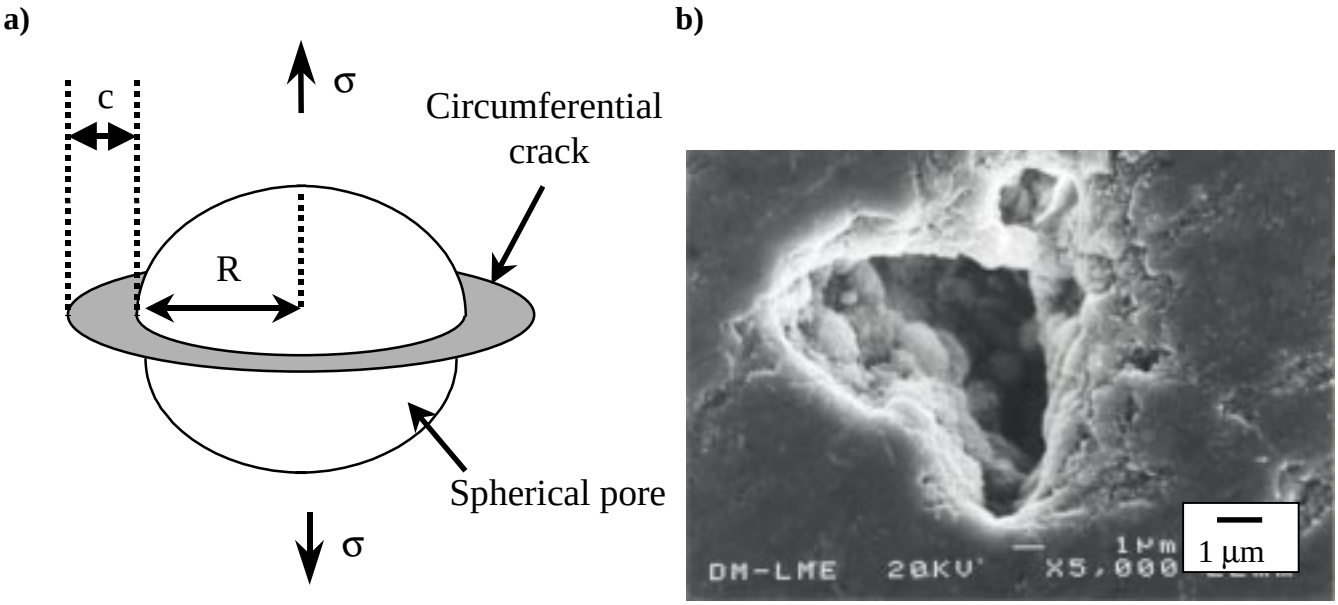

Figure 1. Schematic description of the pore-crack defect. (b) SEM micrograph of pores.

- The tangency between the R-curve and the applied stress intensity factor defines the stress level and crack extension triggering unstable fracture. Various studies are available on the stress intensity factor of a circumferential crack emanating from an embedded spherical pore [5, 6]. For simplicity, the relation between the normalized stress intensity factor and c/R in figure 4 of Ref. 5 is fitted to the following equation:

$$K_{ap} = 1.12 \frac{2.51 + 2.34\, c/R}{1 + 3.87\, c/R}\, \sigma_f \sqrt{\pi c} \qquad (2)$$

The factor 1.12 is introduced to account for the case when fracture is triggered by pores located at the free surface of the specimen (it can be set equal to 1 in the event that failure is confirmed to originate from pores located away from the free surface of the specimen), and σ_f is the fracture stress.

- The R-curve is influenced by the crack geometry, since for a given transformation zone height, the amount of crack shielding would depend on crack shape. Thus, the R-curve used in the fracture model is evaluated with semielliptical cracks, that is, with a shape similar to that of natural cracks [3].

- Shielding effects due to crack loading history are disregarded. It is assumed that a transformation zone is not present around the initial cracks emerging from pores. Hence, the transformation zone develops gradually by the application of external loads. This simplifies the fracture model, as the assessment of crack growth with a preformed transformation zone would depend on the way load was applied during the early growth of the crack (crack loading history). In the case of the studied Y-TZP, this consideration is reasonable in light of the low transformation capability of the material. Further, it is in agreement with the assumption that cracks nucleate upon cooling to room temperature after sintering.

- Strength distribution follows the Weibull model. Thus, the fracture probability, P_f, of a solid subjected to a homogeneous tensile stress, is given by

$$P_f = 1 - \exp\left[-\left(\frac{\sigma_f}{\sigma_0} \right)^m \right] \tag{3}$$

where σ_0 and m are constants which rule the fracture distribution. The parameter m is commonly referred to as Weibull modulus and accounts for strength variability, i.e. the higher the m, the narrower the strength distribution.

- Fracture is triggered by the largest pore size present at the surface of the specimen, where the maximum stress is operating. For a distribution function *g(R)* (see figure 2), which gives the probability that a pore size, R, is present in a unit volume of material, the probability (F) that pores larger than R_i are present in such volume is calculated as:

$$F = \int_{R_i}^{\infty} g(R)dR \,. \tag{4}$$

Consequently, the fracture probability, $P_{f,i}$ is also given by the Eqn. (4). Being this the case, the survival probability, $P_{s,i,}$ ($P_{s,i,}=1-P_{f,i}$), of a generic volume of material, V, (where $V=nV_0$) is then equal to $P_{s,i}^n$. Thus:

$$P_{s,i} = \left(1 - \int_{R_i}^{\infty} g(R)dR \right)^n \tag{5}$$

By noting that for any number κ, $(1-\kappa/(V/V_0)) \sim e^{-\kappa}$ when $V>>V_0$, it follows from Eqn. (5) that $P_{f,i}$ may be written as:

$$P_{f,i} = 1 - \exp\left(-\frac{V}{V_0} \int_{R_i}^{\infty} g(R)dR \right) \tag{6}$$

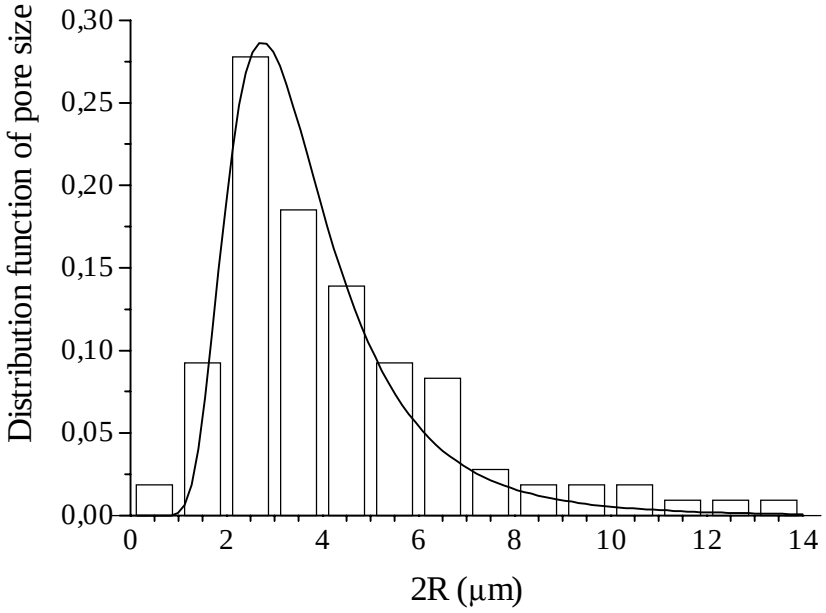

Figure 2: Pore size distribution, in terms of g(R) function.

RESULTS AND DISCUSSION

The model presented above enables the calculation of fracture strength variability from the pore size distribution. As indicated in the aforementioned assumptions, the tangency condition ($K_{ap}=K_r$) yields the fracture strength for a given pore size provided the ratio c/R is known a priori. Hence, in order to compute the fracture strength distribution, the value c/R was calibrated in the present work by establishing from SEM observations the size and location of the pores leading to fracture in three different specimens. As the fracture load was recorded for each of these specimens, it is possible to compute the actual stress level to which each of the pores was subjected, and to estimate the effective value of c. Such calculation gives values of the initial crack length, c, between 0.9 and 1.0 μm.

From the pore size distribution function showed in figure 2 and Eqns. (3)-(5) the fracture strength distribution is calculated. The results are shown in figure 3 together with the experimentally measured strength distribution under three-point bending. It is found that the computed value of m=13.5 is quite similar to that measured under three-point bending (see table 1), and that the influence of c/R in such estimation is relatively mild as it mostly affects the characteristic strength, σ_0, of the distribution.

TABLE 1
FRACTURE PARAMETERS MEASURED EXPERIMENTALLY
AND COMPUTED FROM THE FRACTURE MODEL.

	σ_f (MPa)	σ_0 (MPa)	m
Experimental	1076 ± 90	1116 ± 95	14.0 ± 0.3
Computations	1381 ± 136	1441 ± 105	13.5 ± 0.5

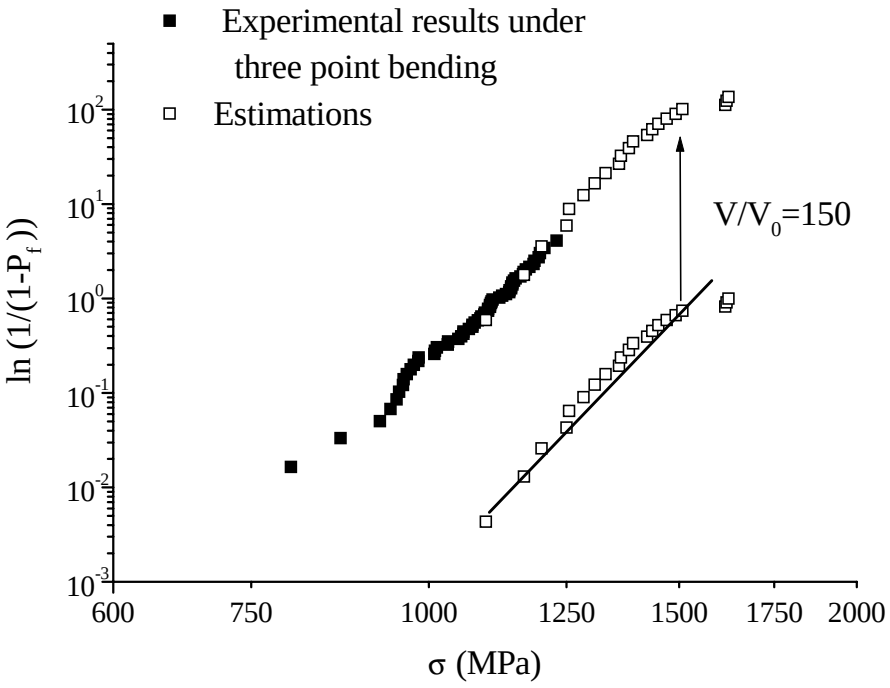

Figure 3: Weibull plots for the experimental results and those computed from the fracture model.

Obviously, the present model does not allow to compute σ_o as this factor depends mostly on the volume of material (V/V_0) that is subjected to tensile loads. Thus, σ_0 varies with the specimen size, its shape and loading conditions. It is emphasized that V/V_0 has to be in the order of 150 so that the computed fracture distribution would match the experimental results under three-point bending. Such value confirms the observations in reference 7 where, by using a similar fracture model, it is indicated that V/V_0 usually ranges from 100 to 1000 in ceramic materials.

With respect to σ_f, it is also expected to depend on the actual volume of the material under tensile loads. For instance, σ_f would be larger for specimens tested under bending loads than for similar specimens subjected to tensile loads as the effective volume of material which carries load in the former is smaller than in the latter case. In addition, loading conditions may determine the type of defects leading to failure. Consequently, surface defects rule fracture strength distribution in bending bars as bulk defects are subjected to comparatively smaller stresses. Under tensile loads, however, defects in different locations throughout the cross section are expected to have a similar importance. In this sense, the fracture origins in the studied Y-TZP were associated to surface pores (as shown in figure 4(a)), in good agreement with the fact that the tests were conducted under bending conditions.

It is noted that in accordance to Weibull statistics, the size of the pores leading to failure is expected to increase as the specimen size increases. This explains the fact that σ_f increases when V/V_0 approaches unity. Simple calculations using Weibull statistics show that under uniaxial loads, the measured strength variability would be shifted to lower stresses by a factor of 0.6 while m remains constant. Such a strength reduction can only be produced by defects which are much larger than those usually encountered in polished surfaces (see figure 4(b)) or, alternatively, by having values of V/V_0 in the order of 10^5. Thus, the correspondence between experimental results and the computed Weibull statistics is difficult to validate experimentally as the pore size distribution would have to be extrapolated into a size range in which a representative number of pores can only be found after extensive measurements with a large number of specimens.

a) **b)**

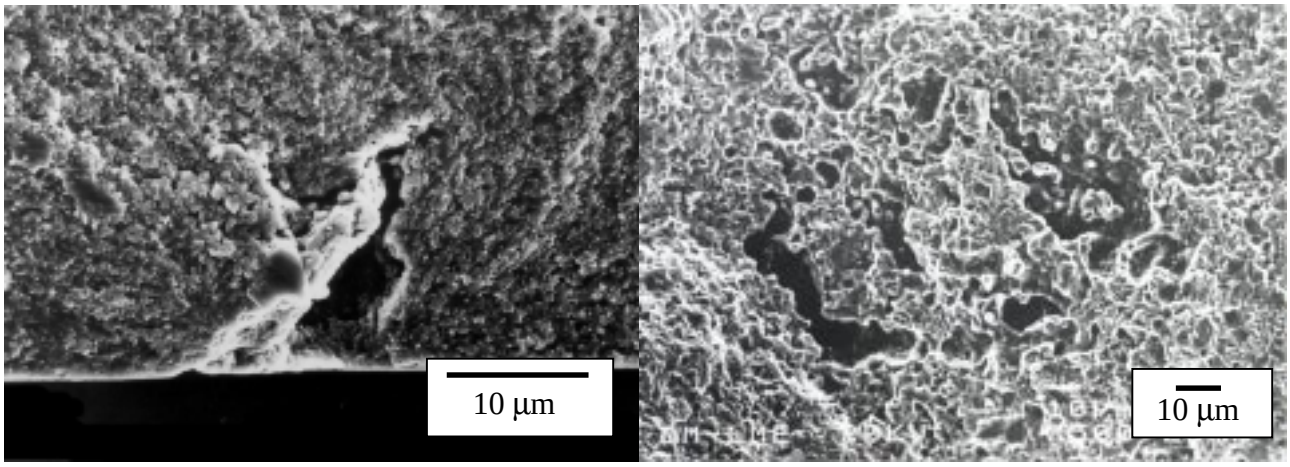

Figure 4: Surface and bulk defect found in fracture surfaces: (a) surface pore that controls the fracture behavior of the material under bending loading. (b) Bulk defect, inactive in the applied load condition.

CONCLUSION

A simplified fracture model is used to compute the fracture strength distribution in a fine-grained Y-TZP, from knowledge of its R-curve behavior and pore size distribution. It is found that material constant m which dictates the fracture variability according to Weibull statistics, can be computed from such fracture model as its value is similar to that measured experimentally. The scaling strength σ_0 of the Weibull statistics depends on the volume of material subjected to tensile loading. Thus, its computation from the fracture model is not direct and requires experimental calibration. Guidelines for such calibration are provided in this paper. Once the agreement between experiments and theory is validated, the fracture model enables the computation of strength variability in a generic ceramic structure.

Acknowledgments

The authors acknowledge the financial support provided by CICYT (Spain) under grant Nº MAT97-0923. The assistance provided by M. Marsal in conducting SEM observations is also acknowledged. One of the authors (D.C.) would express his gratitude to the Generalitat de Catalunya for the scholarship received.

REFERENCES

1 Rice R.W., *J. Mat.Sci.*, **19** (1984) 895.
2 Govila R., *J. Mat. Sci.*, **30** (1995) 2656.
3 Casellas D., Alcalá J., Llanes L. and Anglada M., submitted to *J. Mat.Sci* (2000).
4 Scubert H., *J. Am. Ceram. Soc*., **69** (1986) 270.
5 Zimmermann A., Hoffman M., Flinn, B.D. Bordia R.K., Chung T.-J., Fuller E.R. and Rödel J., *J. Am. Ceram. Soc*., 81 (1998) 2527.
6 Fett T., *Int. J. Fract*., **67** (1994) R-41.
7 Danzer R. and Lube T. (1996), *Fracture Mechanics of Ceramics 11*, pp 425-32, Bradt et al. (Eds). Plenum Press, NY, USA.
8 Stanley P., Fessler H. and Sivill A.D., *Proc. Brit. Ceram. Soc*., **22** (1973) 453.